Genomics 96 (2010) 134–145

Contents lists available at ScienceDirect

Genomics

journal homepage: www.elsevier.com/locate/ygeno

Genomic phenotype of non-cultured pulmonary fibroblasts in idiopathic pulmonary fibrosis

Margaret C. Emblom-Callahan [a], Mantej K. Chhina [a], Oksana A. Shlobin [b], Shahzad Ahmad [b], Erika S. Reese [a], Eswar P.R. Iyer [a], Daniel N. Cox [a], Renee Brenner [b], Nelson A. Burton [b], Geraldine M. Grant [a,*], Steven D. Nathan [b]

[a] George Mason University, Department of Molecular and Microbiology, 10900 University Blvd., Manassas, VA 20110, USA
[b] Inova Fairfax Hospital, Inova Advanced Lung Disease and Lung Transplant Program, 3300 Gallows Road, Falls Church, VA 22042, USA

ARTICLE INFO

Article history:
Received 29 January 2010
Accepted 29 April 2010
Available online 6 May 2010

Keywords:
Idiopathic pulmonary fibrosis
Fibroblast
Microarray
Genomics

ABSTRACT

Activated fibroblasts are the central effector cells of the progressive fibrotic process in idiopathic pulmonary fibrosis (IPF). Characterizing the genomic phenotype of isolated fibroblasts is essential to understanding IPF pathogenesis. Comparing the genomic phenotype of non-cultured pulmonary fibroblasts from advanced IPF patients' and normal lungs revealed novel genes, biological processes and concomitant pathways previously unreported in IPF fibroblasts. We demonstrate altered expression in proteasomal constituents, ubiquitination-mediators, Wnt, apoptosis and vitamin metabolic pathways and cell cycle regulators, suggestive of loss of cellular homeostasis. Specifically, *FBXO32, CXCL14, BDKRB1* and *NMNAT1* were up-regulated, while *RARA* and *CDKN2D* were down-regulated. Paradoxically, pro-apoptotic inducers *TNFSF10, BAX* and *CASP6* were also found to be increased. This comprehensive description of altered gene expression in isolated IPF fibroblasts underscores the complex biological processes characteristic of IPF and may provide a foundation for future research into this devastating disease.

Introduction

Idiopathic pulmonary fibrosis (IPF) is a fatal form of interstitial lung disease (ILD) of unknown etiology, with an associated median survival time of approximately 3 to 5 years from the time of diagnosis [1]. There is no effective medical treatment or cure for IPF. The purported effector cells of this devastating disease are the fibroblasts, predominantly evident in distinct fibrotic foci in the diseased lung. These activated fibroblasts are largely felt to be responsible for the production of the extracellular matrix (ECM), which forms the nidus for subsequent fibrosis with the resulting pathological, radiographic and clinical sequelae that characterize the disease [2].

The purported pivotal role of the pulmonary fibroblast in the pathophysiology of IPF and the absence of effective therapies underscore the necessity for a thorough molecular characterization of this cell. This will enable a better understanding of the etiology and triggers of this disease and guide potential therapeutic strategies. To date there are no high through-put genomic analysis studies that specifically characterize global expression changes of this cell in isolation prior to *in vitro* propagation, or in comparison to its normal fibroblast counterpart. Thus far, studies have provided useful insights into the global genomic profile of the whole IPF lung. Specifically, the genomic profile of IPF whole lung tissue has been compared to other ILDs, including hypersensitivity pneumonitis and non-specific interstitial pneumonitis (NSIP) [3]. In addition, studies have also investigated the differential gene expression in familial versus sporadic IPF [4].

Therefore, in this study, we set out to characterize the genomic profile of non-cultured IPF fibroblasts in isolation to characterize the specific contribution of this cellular component to this disease. Specifically, the gene expression profiles of IPF fibroblasts were compared to normal fibroblasts, using an oligo-microarray representing 33,791 transcripts from the Ensembl Human Build (BI-35C) including 22,169 unique genes (Operon's Human Oligo Set, version 4.0). This is the first report of a direct comparative analysis of non-cultured IPF fibroblasts to non-cultured normal pulmonary fibroblasts. The fibroblasts used in this study were isolated immediately post-lung explantation, and were not subjected to long-term *in vitro* propagation. This immediate isolation therefore bypassed the dedifferentiating effects of long-term tissue culture and preserved, as closely as possible, the cells' *in vivo* phenotype.

Our investigation of the genomic aberrations of IPF fibroblasts gives insight into the biological processes that characterize this disease. This comprehensive characterization of the fibroblast's

* Corresponding author. 10900 University Blvd., 4D7, Manassas, VA 20110, USA. Fax: +1 703 993 9009.
E-mail address: ggrant1@gmu.edu (G.M. Grant).

0888-7543/$ – see front matter © 2010 Elsevier Inc. All rights reserved.
doi:10.1016/j.ygeno.2010.04.005

genotype will hopefully provide a platform and a roadmap for future studies into the pathogenesis and treatment of this deadly disease.

Materials and methods

We performed a prospective, comparative gene expression analysis of fibroblasts isolated from the lung tissue of 12 patients with advanced IPF and 6 normal controls (Table 1). IPF lung tissue was obtained through Inova Fairfax Hospital (VA). All normal control lungs were obtained through the Washington Regional Transplant Community (WRTC). Statistical significance for the demographic values of the two groups was determined by unpaired *t*-test using Graph Pad Prism 4.0 software. This study was approved by the Inova Fairfax Hospital Internal Review Board and the George Mason University Human Subject Review Board.

Specimen procurement/dissection

Both IPF and normal lungs were procured in the operating room within minutes of explantation. To ensure a consistent and equivalent comparison, we oriented each lung from the apex to base, and isolated samples from four discrete regions: peripheral, central, upper and lower.

Post-dissection processing

We isolated the fibroblasts by differential binding after enzymatic dissociation as previously described in Wang [5]. Specifically, all samples were dissected into 1–2 mm^2 pieces at 4 °C in PBS and subjected to enzymatic digestion in 0.4% collagenase P (Roche, Indianapolis, IN) in complete media (Dulbecco Minimum Essential Media (DMEM) containing 10% fetal bovine serum (FBS), penicillin (100 I.U./mL), streptomycin (100 MCH/mL), amphotericin B (0.25 M.C.G/mL) (P/S/A)) and 0.1% DNase1, final concentration at 37 °C in a humidified 5% CO_2 incubator for 2 h. The resulting digested material was passed through a sterile fine mesh to remove undigested tissue, and cells were collected by centrifugation at 1000 *g* for 5 min. The pelleted cells were re-suspended in complete media and seeded onto tissue culture treated plastic (glass slides for immunocytochemistry) at 37 °C and 5% CO_2 for 45 min. At 45 min the attached fibroblast cells were washed vigorously with sterile PBS and flash frozen for RNA extraction or fixed for immunocytochemistry.

Morphology of cell populations

Morphological analysis was carried out by phase contrast light microscopy. Non-cultured IPF and normal fibroblasts were imaged at the 45 min attachment time-point, post-isolation. After 120 h *in vitro*, the morphological effect of long-term culture was observed and recorded.

Table 1
Demographics of IPF and normal donors.

Variable		IPF patient ($n=12$)	Normal ($n=6$)	*p*-value
Age		60.9 (±7.2) years	50.8 (±18.1) years	0.12
Sex	Male	7	3	0.75
	Female	5	3	
Smoking history (no current smokers)	None	2	6	<0.01
	Past	10	0	
Race	African American	2	2	0.45
	Caucasian	10	4	

Identification of cell populations

The fibroblast identity of these cells was confirmed by immunocytochemistry both in the 45 min differential binding population and this same population continued in long-term cell culture for 120 h. Positive control cells included A549 (epithelial, human), microvascular endothelial cells (endothelial, human) and MD (macrophage, human) (ATCC, Rockville, MD). Briefly, fixed cells (50/50% Acetone/Methanol (v/v) at −20 °C) were blocked in blocking buffer (BB) (1× PBS with 0.3% Triton-X 100 (1× PBST) and 5% normal goat or donkey serum) for 30 min at room temperature, followed by overnight incubation at 4 °C in BB containing the primary antibodies as follows: anti-human actin, alpha 2, smooth muscle, aorta (αSMA)(Abcam #Ab7817; fibroblast), anti-human cytokeratin 18 (K18)(AbCam #Ab668; epithelial), anti-human CDllb (AbCam #Ab52478; monocyte/macrophage) and anti-human Von Willebrand's Factor (Ab68545; endothelial). The cells were then rinsed in 1×PBST (3×10 min) and incubated with secondary antibody: goat anti-mouse conjugated with Texas red (AbCam #6787) or donkey anti-rabbit conjugated with Texas red (AbCam #6799), for 2 h at room temperature. The cells were then incubated with DAPI (5 mg/mL) in dimethylformamide for 2 min, and finally mounted in 80/20% glycerol/PBS (v/v). Immunofluorescent images were captured using a Nikon C1 confocal system mounted on a Nikon Eclipse 90i microscope. Images were processed using Nikon EX-C1 imaging software and Adobe Photoshop 4.0.

To determine the percentage of positively stained cells, the total number of cells was counted in 5 random fields in addition to the total number of positive cells for each antibody and the percent determined.

Microarray analysis

RNA was extracted using a Qiagen RNeasy kit (Qiagen, Valencia, CA) and DNase was treated using DNase free (Ambion, Austin, TX). The quality and quantity of the RNA was determined using RNA 6000 nanochips and an Agilent Bioanalyzer. For microarray analysis, 1 μg of RNA was amplified and amino-allylated using the MessageAmp II aRNA kit (Ambion). All microarrays were carried out by the Duke Institute for Genome Sciences and Policy, Microarray Facility using HO36K human chip (Operon Human Oligo set V4), and two color amino-allylated amplified RNAs: cy5 patient and normal samples, and cy3 Stratagene human reference RNA.

All analyses of the resulting genepix files was carried out using the TM4 software suite (ExpressConverter V1.0, MIDAS, MEV) and normalized by locally weighted linear regression (lowess) [6,7]. Normalized, filtered (percent filter cut-off 60%) data was statistically analyzed using statistical analysis of microarray (SAM) [8]. Data was independently confirmed using Mann–Whitney Analysis Benjamini–Hochberg step-up procedure (Data not shown). A final list of 1813 transcripts including 1480 unique genes was derived, with a False Discovery Rate (FDR) set to 0%. Significant transcripts were then clustered by Euclidean distance hierarchical clustering using average linkage.

MIAME compliance

The data discussed in this publication have been deposited in NCBI's Gene Expression Omnibus in fulfillment of MIAME compliance requirements and are accessible through the following link: http://www.ncbi.nlm.nih.gov/geo/query/acc.cgi?token=bnwnzkcamugmkdq&acc=GSE17978.

Confirmation of gene expression analysis

Quantitative real time reverse transcriptase polymerase chain reaction (qRT-PCR)

The direction and fold change of representative genes identified by microarray analysis was confirmed by qRT-PCR. DNase treated unamplified RNA (1 μg) was reverse-transcribed to cDNA using an iScript cDNA synthesis kit (Bio-Rad, Hercules, CA). qRT-PCR was carried out using Quantifast SYBR Green PCR Kit (Qiagen). Primers were selected *de novo* or from previous publications (Table 2), and samples were carried out in triplicate and normalized to 18S expression levels using the delta delta CT method [9].

Multiple criteria were used to select genes for expression confirmation. Genes associated with significantly represented biological processes were chosen including a selection of randomly chosen genes to prevent investigator bias. A combination of genes that were up-regulated as well as down-regulated, and genes whose expression changes showed higher magnitude of change as well as genes with smaller expression changes were included.

Western analysis of protein levels

Total cellular protein was isolated from the non-cultured IPF and normal fibroblasts using RIPA buffer (Pierce, Rockford, IL), with addition of mini-complete protease inhibitors (Roche). The total protein concentration was determined using the Bradford assay (Bio-Rad). For western analysis, 30 μg of total protein for each sample was subjected to electrophoresis in a 4–12% Bis-Tris gradient gel (Invitrogen, Carlsbad, CA). Transfer was carried out using the iBLOT system (Invitrogen) and nitrocellulose membranes. Owing to the documented instability of loading controls in primary lung tissue, to ensure equal loading, all lysates were subjected to a) triplicate independent Bradford assay to ensure accurate quantification of protein concentration, b) Coomassie Blue staining of gels to visualize and verify equivalent protein loading (Simply Blue solution (Invitrogen)), and c) 1% Ponceau S staining (Sigma, St. Louis, MO) of transfer membrane for total protein transferred. Membranes were blocked in 5% (w/v) non-fat dried milk in 1× Tris-buffered saline containing 0.1% tween-20 (TBST) for 1 h at room temperature, and then incubated overnight at 4 °C with primary antibody in TBST. Following primary incubation, membranes were washed and then incubated with HRP-linked secondary antibodies (Abcam) for 1 h at room temperature. Immuno-blot membranes were visualized by incubation with SuperSignal West Femto Max Sensitivity Substrate (Pierce) and imaged using a ChemiDoc XRS™ System (Bio-Rad) with Quantity One Software (Bio-Rad). Bands were quantified using the Quantity One Software (Bio-Rad) in triplicate for each antibody. The following primary antibodies were used: actin, alpha 2, smooth muscle, aorta (ACTA2; AbCam#7817), Bax (Cell Signaling #2774), CASP8 and FADD-like apoptosis regulator (CFLAR; AbCam #4042), fibroblast activation protein, alpha (FAP; AbCam#54651), glyceraldehyde-3-phosphate dehydrogenase (GAPDH; AbCam #8245), matrix metallopeptidase 11 (MMP11; AbCam#52904), phosphatase and tensin homolog (PTEN; Cell Signaling #9552; Cell Signaling, Danvers, MA), periostin (POSTN; AbCam #14041), tumor necrosis factor receptor superfamily, member 1A (TNFRSF1A; AbCam #19139), tumor necrosis factor receptor superfamily and member 10D (TNFRSF10D; AbCam #2019).

Statistical analysis of altered protein levels

Graph Pad Prism 4.0 software was utilized to calculate statistical significance of altered protein abundances across three biological replicates of both IPF and normal samples. Each immunoblot was repeated in triplicate, and technical replicates for each biological sample were averaged. The data were normally distributed; therefore, an unpaired *t*-test was used to calculate statistical significance of densitometry readings obtained through band analysis using Quantity One Software (Bio-Rad).

Analysis of biological processes

Pathway and gene ontology analyses were carried out using *D*atabase for *A*nnotation, *V*isualization and *I*ntegrated *D*iscovery (DAVID) available online through the National Institute of Allergy

Table 2
qRT-PCR primers and amplicon lengths used to verify observed microarray expression changes.

Gene symbol	Forward primer	Reverse primer	Amplicon length
18S	GATGGGCGGGGAAAATAG	GCGTGGATTCTGCATAATGGT	165
BAX	GGGTGGTTGGGTGAGACTC	AGACACGTAAGGAAAACGCATTA	191
CCNH	TGTTCGGTGTTTAAGCCAGCA	AGTGAGCATTATTATCCTGGGGT	120
CD40	AGACACCTGGAACAGAGAGAC	AACCCCTGTAGCAATCTGCTT	211
CFL1	TTCAACGACATGAAGGTGCGT	TCCTCCAGGATGATGTTCTTCT	110
CNN1	ATGTCCTCTGCTCACTTCAACC	CCCCCTCGATCCACTCTCT	121
CNN2	ACCGGCTCCTGTCCAAATATG	CCCGGCTGTAGCTTGTTCA	151
CNN3	AGAAGAGGTGACAGGCATGAG	GAGGCCAGTTCAGTGAGGAC	137
CXCL12	ATGCCCATGCCGATTCTTCG	GCCGGGCTACAATCTGAAGG	101
CXCL14	CGCTACAGCGACGTGAAGAA	TTCCAGGCGTTGTACCACTTG	170
FN1	GAAGCTCTCTCTCAGACAACCA	GCCCACGGTAACAACCTCTT	234
HDAC2	ATGGCGTACAGTCAAGGAGG	TGCGGATTCTATGAGGCTTCA	112
IL1R2	TTCGTGGGAGGCATTACAAGC	ACCGTCCTAGCAGAGTCATTT	145
ITGB5	AAGTTGTTTCCAAATTGCGTCC	CTTTCGCCAGCCAATCTTCTC	186
KIT	GTTCTGCTCCTACTGCTTCGC	CCACGCGGACTATTAAGTCTGA	115
MMP1	ACACATCTGACCTACAGGATTGA	GTGTGACATTACTCCAGAGTTGG	103
MMP11	TCTACACCTTTCGCTACCCAC	CTCCAGCGGTGCAATCTCATT	152
MMP2	CTTCCAAGTCTGGAGCGATGT	TACCGTCAAAGGGGTATCCAT	119
MMP25	GACTGGCTGACTCGCTATGG	CGAACCTCTGCATGACTTTGATG	106
PSMA2	ACCAAGAACCCATTCCTACAGC	GTCCCTCATTCCAACCACAAAT	126
PXN	CCTGGAGCAAAGAGCGGATG	CCCCCAGCTTGTTCAGGTC	209
RAN	GGTGGTACTGGAAAAACGACC	AACACTAGGGGATGAACCTCAA	101
STAT5B	GAGGTGCGGCATTATTTATCCC	CAGCGGTCATACGTGTTCTGG	218
SIPA1	CCCTAAGGGAACTCCAAAATCTG	CGGTTGTTGTGTCTCAGGC	168
SPP1	TCACCAGTCTGATGAGTCTCAC	CAGGTCTGCGAAACTTCTTAGAT	182
TFDP1	TGAAGCCAACGGAGAACTCAA	GCGTACCAATTACCACTTGCTG	176
THY1	TCGCTCTCCTGCTAACAGTCT	CTCGTACTGGATGGGTGAACT	134
TNFRSF14	ACCCTGTGTCAGAACTGCC	GGCTCCCTGAGAGAAACCAC	151
TNFRSF1a	TGGTGGGAATATACCCCTCAG	GCACTTGGTACAGCAAATCGAAT	131
USP19	CAGGACTGGAGGACACCACTA	GAGGCCAGAGGTTCAAGACC	130

and Infectious Diseases (NIAID) [10,11]. The official gene symbols were entered into the DAVID database and the resulting gene ontologies were analyzed for enrichment of biological processes. Additional pathway analysis was carried out through Kyoto encyclopedia of genes and genomes (KEGG) [12–14].

Results/discussion

Cell population

Our model of non-cultured isolated fibroblasts was central to this study's design. Specifically, the fibroblasts used in this study were extracted expeditiously from explanted lungs, which limited *ex vivo* phenotypic transformations known to occur as a result of *in vitro* propagation of primary cells and tissue explants [15–17]. The technique of differential binding has successfully been used previously to both isolate and eliminate fibroblasts [5,18–20], however this is the first report of fibroblasts isolated in this manner from lung tissue without subsequent long-term tissue culture.

Immediately post-isolation, both the IPF and normal fibroblasts shared a rounded morphology (Figs. 1A and C). However, when continued in culture over 120 h, both cell populations demonstrated the classic fibroblast-like elongated morphology (Figs. 1B and D) and extensive α-SMA staining (Figs. 1F and H). Further immunocytochemical analyses clearly demonstrated that both the IPF and normal fibroblasts were virtually free of contaminating epithelial cells (Figs. 2A and C), monocytes/macrophages (Figs. 2D and F) and endothelial cells (Figs. 2G and I). Quantification of K18 and α-SMA staining of IPF and normal fibroblast populations immediately post-isolation both demonstrated that IPF and normal fibroblasts were virtually free of contaminating epithelial cells and confirmed the fibroblast identity of the cells. Specifically, both cell populations demonstrated negligible presence of the epithelial cell marker, K18, ($1.80 \pm 0.67\%$), and stained positively for α-SMA ($99.80 \pm 0.24\%$) immediately post-isolation, tested in five randomly chosen fields.

Microarray analysis

To determine the differential gene expression between non-cultured IPF and normal fibroblasts, we extracted RNA from fibroblasts isolated as described. A total of 38 samples from 12 IPF lungs and 19 samples from 6 normal lungs were analyzed (Table 1). SAM analysis (FDR = 0%; delta = 2.26) identified 1813 significantly differentially expressed transcripts between IPF fibroblasts and normal fibroblasts. Hierarchical clustering (Euclidean distance) revealed a clear distinction between the IPF and normal fibroblasts across all samples, highlighting the significant distinction in global gene expression between these two unique fibroblast populations.

Validation of the microarray results

Validation of transcript abundance

Microarray data was validated using qRT-PCR of selected genes from the gene list. In each case qRT-PCR fold changes correlated with those derived from the SAM analysis (Table 2, Fig. 3).

Validation of translation into proteins

Western blot analysis was used to determine the altered abundance of 12 selected proteins represented in our microarray data. All alterations in protein abundance coincided with the directional changes of genes identified through the microarray analysis (Figs. 4A and B).

Biological processes identified in IPF fibroblasts—DAVID and KEGG analyses

DAVID analysis of our 1813 significant-genes list derived a comprehensive ranking of functional annotations and ontologies. Of the significantly altered transcripts, 1242 unique genes were recognized and categorized by DAVID (Table 3). This analysis described many altered biological processes and constituent pathways (Table 4) previously unreported in IPF fibroblasts. Specifically,

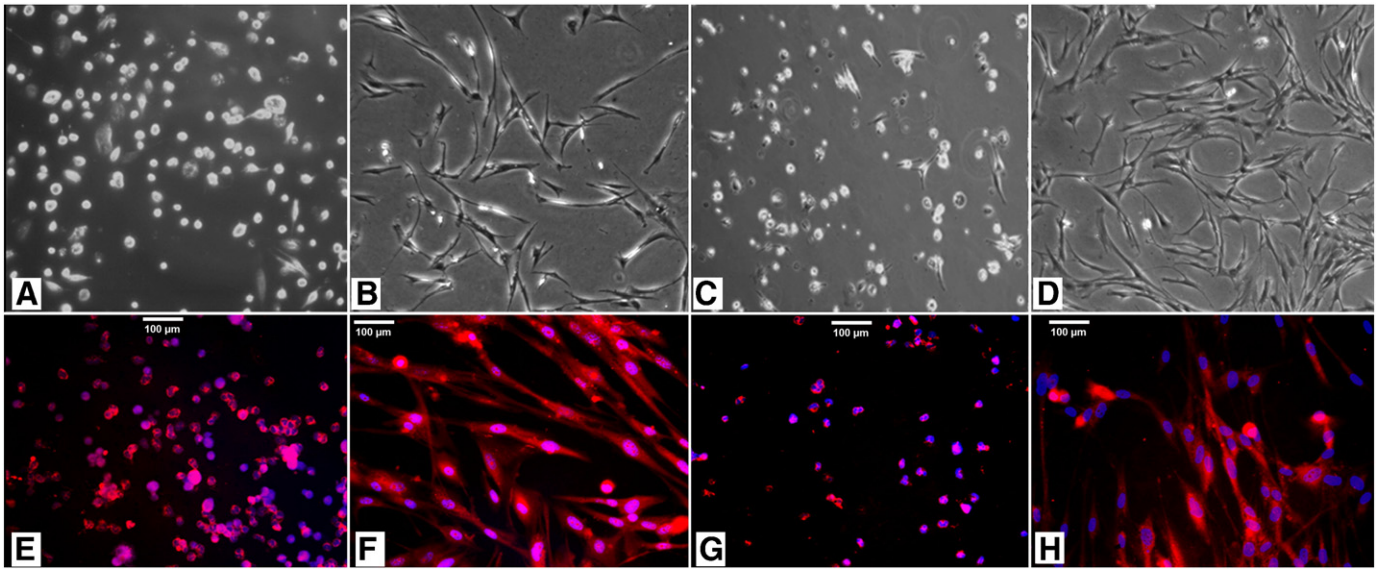

Fig. 1. Confirmation of IPF and normal fibroblast cell populations. Morphology of IPF fibroblasts and normal fibroblasts at 45 min differential binding appears rounded (A and C) (100× magnification imaged on a Leica light microscope). After 120 h in culture, these cells acquire the familiar stretched-out fibroblast-like morphology (B and D). Immunofluorescent staining of IPF fibroblasts (E) and normal fibroblasts (G) at 45 min differential binding demonstrates the presence of alpha smooth muscle actin (Texas Red and DAPI nuclear stain, 200× magnification). The 45 min differential binding population continued in culture for 120 h, IPF fibroblasts (F) and normal fibroblasts (H) show diffuse and characteristic staining for alpha smooth muscle actin depicting the stress fibers (200× magnification). Size bar set to 100 µm.

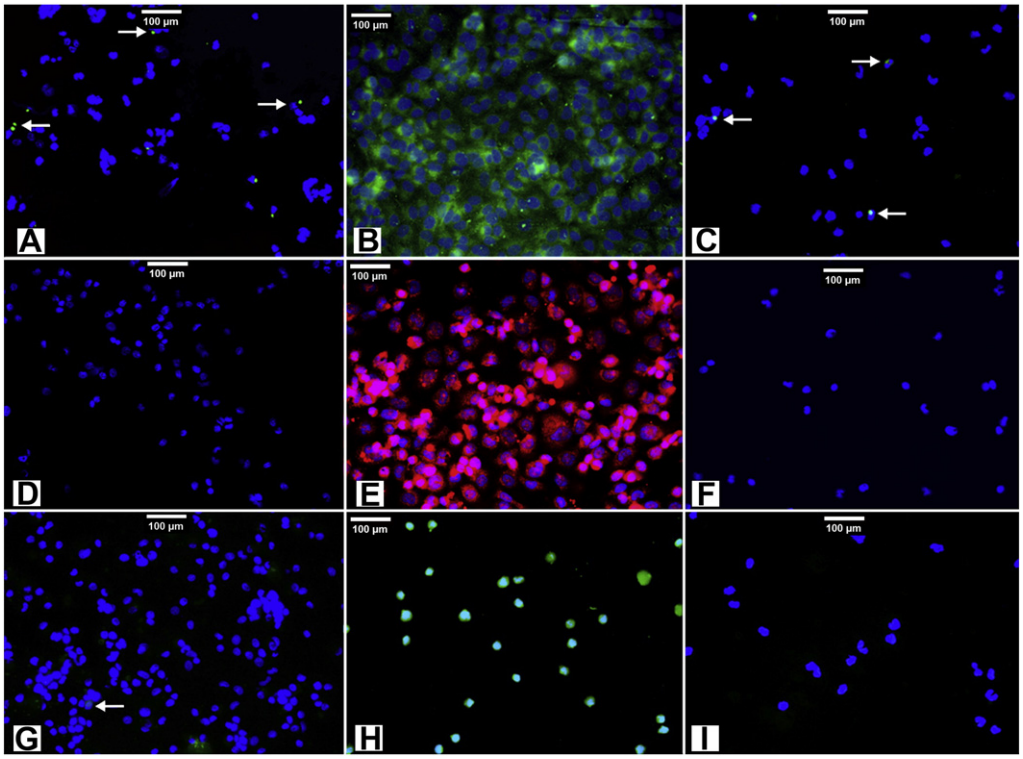

Fig. 2. IPF and normal fibroblast cell populations demonstrate negligible cellular contamination. Immunofluorescent staining of IPF fibroblasts (A) and normal fibroblasts (C) for cytokeratin 18 epithelial cell marker (conjugated to Texas Red (green pseudo-color) and DAPI nuclear stain; 200× magnification) shows very few positive cells (arrows). (B) A549 pulmonary epithelial cells, positive control for cytokeratin 18. Immunofluorescent staining of IPF fibroblasts (D) and normal fibroblasts (F) depicts the absence of staining for endothelial cell marker, Von Willebrand's Factor (conjugated to Texas Red (pink pseudo-color) and DAPI nuclear stain) compared to human microvascular endothelial cells, positive control (E). Immunofluorescent staining of CD11b, monocyte/macrophage cell marker (conjugated to Texas Red (green pseudo-color) and DAPI nuclear stain; 200× magnification), depicts few potential contaminants in the IPF fibroblast population (G) and normal fibroblast population (I) compared to human monocyte/macrophage cell line, MD (H). Size bar was set to 100 µm.

unique to this study was the identification of alterations in catabolic processes including the ubiquitin/proteasomal degradome and vitamin metabolism. In support of the validity of our data, we also identified a number of biological processes and representative pathways previously reported in association with IPF lungs. The nature of this analysis within the context of this isolated and non-cultured cellular population enables us to attribute these biological processes specifically to the fibroblast cell populations. Of these processes, cell death associated processes ranked highest in significance, while other biological processes, some of which have previously reported to be associated with IPF fibroblasts, were also identified. These included wound healing and response to stress processes [21,22]; cytokine receptor signaling including chemokines, tumor necrosis factor-α (TNF-α) and transforming growth factor-β (TGF-β) signaling members [21–24]; the Wnt pathway [24–26]; ECM–receptor interactions [27]; cytoskeletal organization and biogenesis [28–30]. These specific important findings are robustly complemented by the global data presented in this study.

Cell death

Within the assemblage of biological processes associated with cell death, we found a complex array of gene alterations involved in apoptosis (Table 3). Interestingly, these included predominantly pro-apoptotic expression changes. Apoptotic dysregulation in IPF is a highly controversial topic. The role that this homeostatic process plays in IPF may be cell-type specific and thereby integral to disease progression. For example, epithelial cells in the IPF lung appear to show increased rates of apoptosis, thereby contributing to loss of lung architecture [31]. On the other hand, while there is data suggestive of an increased rate of apoptosis in IPF fibroblasts derived from lung tissue explants [32], other studies suggest that IPF fibroblasts are more apoptosis resistant [31–33]. There is also a disparity between previous findings of decreased apoptosis and our data, which suggests a preponderance of pro-apoptotic expression changes. This discrepancy may be attributable to the nature of the fibroblasts used in this study, which were non-cultured. For example, we found increased expression of the apoptosis inducing ligand *TNFSF10* (TRAIL ligand) and concurrent down-regulation of its decoy receptor, *TNFRSF10D.* This decoy receptor interacts with TNFSF10, but lacks the apoptosis inducing death domain which would suggest an increased propensity for apoptosis in fibroblasts. The expression of other downstream pro-apoptotic mediators was also altered in IPF fibroblasts, including up-regulation of *BAX* (Figs. 3C and 4) and pro-apoptotic *CASP6*. Additionally, down-regulation of the pro-survival interleukin-1 receptor-associated kinase 1 (*IRAK1*) was also observed adding to the overall potentially pro-apoptotic signaling environment. This data would seem to be in opposition to the overall abundance of fibroblasts in the IPF lung. However, the complex milieu that is the IPF lung undoubtedly plays a role in modulating these signals. In light of these complexities, our data suggest that an in-depth investigation of apoptotic signaling in each cell type in the IPF lung may unravel this conundrum.

Catabolic processes

Within the data for IPF fibroblasts was a significant representation of catabolic processes which may provide insight into dysregulated homeostasis in these cells. In IPF, conflicting signals for massive ECM deposition are pitted against those for ECM and protein degradation. This involves proteases such as the matrix-

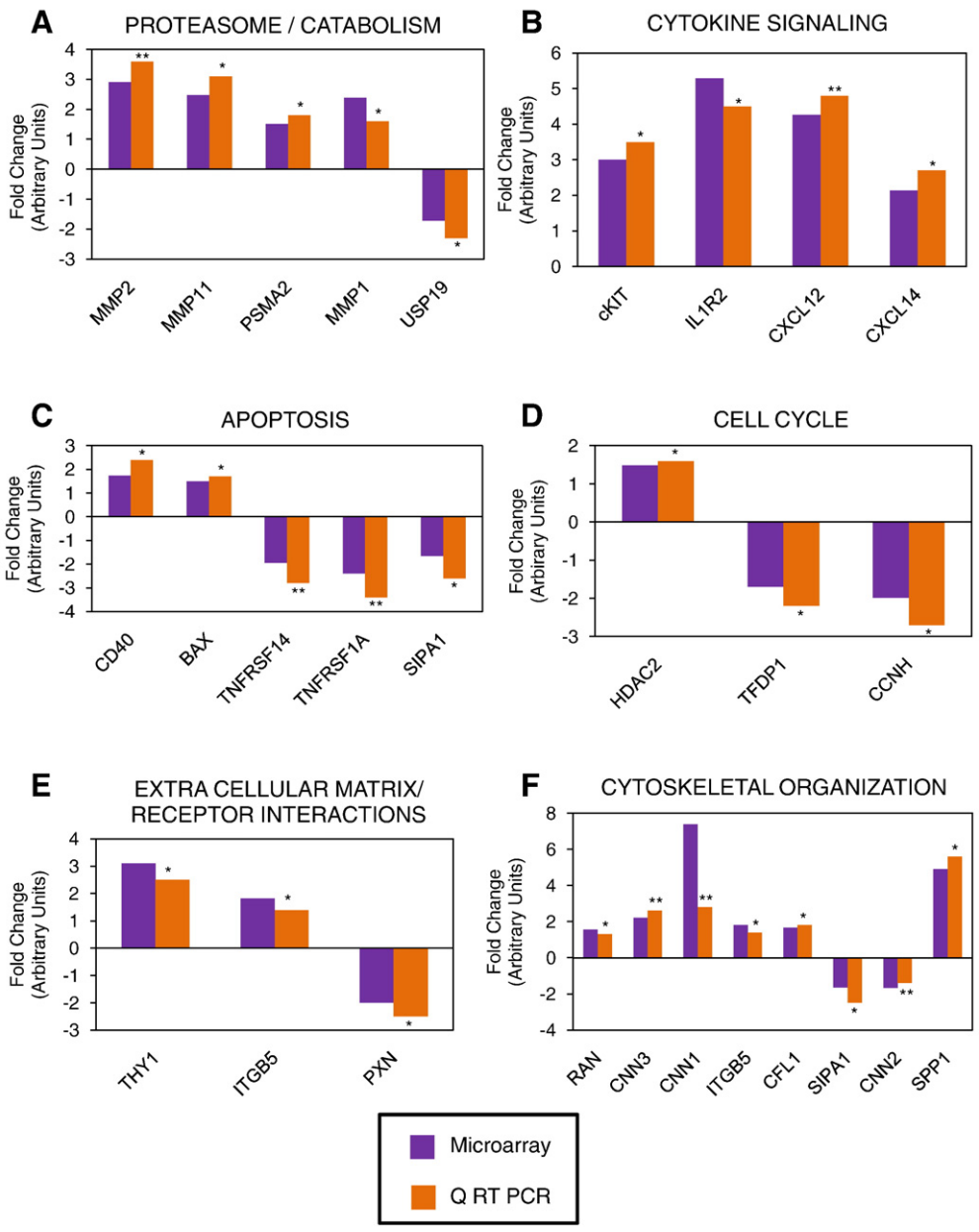

Fig. 3. qRT-PCR confirmed the direction and further elucidated the fold change (arbitrary units) of selected genes identified in the microarray analysis. (* = $p<0.05$ and ** = $p<0.01$.)

metallopeptidases (MMPs), a disintegrin and metalloproteinase (ADAMS) and their inhibitor proteins, tissue inhibitors of metalloproteinases (TIMPS). This complex interplay between these catabolic and anabolic enzymes has been dubbed the degradome. It has been suggested that in IPF this degradome is abnormal, resulting in deregulation of the catabolic processes inherent to cellular homeostasis [34]. Within the biological processes that encompass catabolism, we identified, for the first time, increased expression of the ubiquitin conjugating enzymes UBE2T, UBE2K and UBE2D4. Additionally de-ubiquitination proteases, such as ubiquitin specific proteases USP6, USP10, USP15, USP18 and USP19 were also altered, as was ubiquitin-like modifier activating enzyme 1 (*UBA1*) (Table 4). These alterations in ubiquitination and de-ubiquitination enzymes potentially have profound implications for ubiquitin/proteosomal regulation and control of proteolysis. This is of particular interest in light of our observation of increased expression of several comõponents of the proteasome including proteasome subunits, PSMB5, PSMA2, PSMA3, and PSMD10. The 26S proteasome is a vast multi-subunit complex, located in the nucleus and cytosol, which accounts for the bulk of cellular protein turnover via ubiquitin tagged degradation [35]. These numerous expression changes noted in the ubiquitin/proteasome regulation of proteins may potentially impact critical homeostatic processes in the IPF fibroblast. For example, with respect to the cell cycle's regulation, we noted increased expression of *FBXO32*, the f-box subunit of the Skp1-Cullin/Cdc53-F-box protein (SCF) complex. The SCF complex is a ubiquitin ligase complex that recognizes sequences in key regulators of cell cycle such as cyclin-dependent kinase inhibitor 1B (CDKN1B; p27, Kip1) and cyclins D, E and A. Altered catabolic regulation in key control elements of the cell cycle that result from this, may dramatically impact proliferation in IPF fibroblasts, and thereby effect an imbalance of cellular homeostasis [36].

Cell cycle

Central to the pathogenesis of IPF, is the control of the cell cycle and the over abundant fibroblast population. Interestingly, in spite of its obvious contribution to the IPF lung phenotype, little research

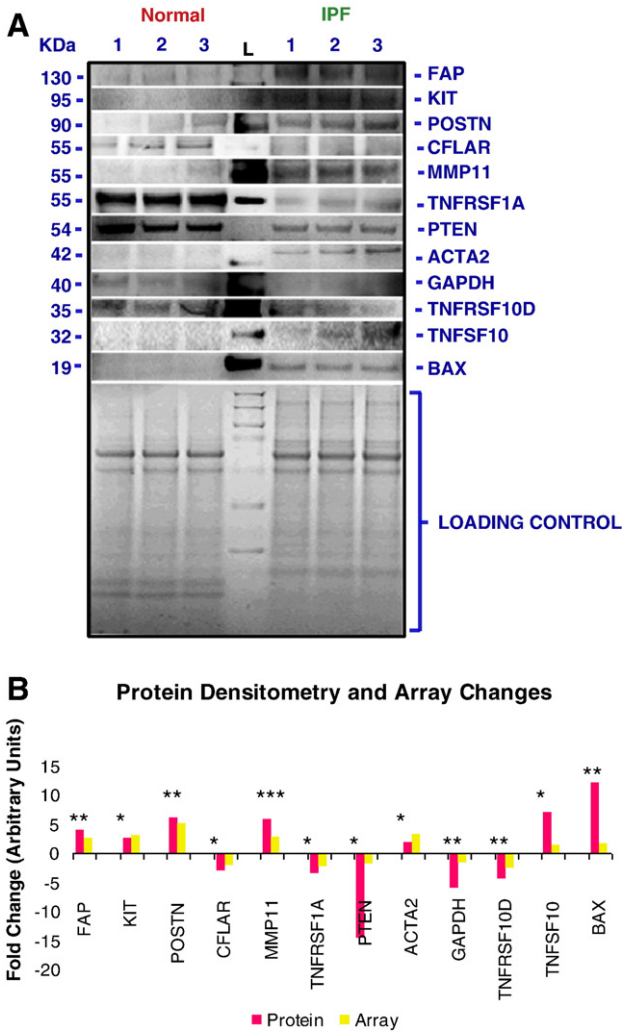

Fig. 4. Immuno-detection of proteins in IPF fibroblasts versus normal fibroblasts. Lanes 1–3 are individual biological replicates of total cell lysates of normal fibroblasts, lane 4 is molecular weight marker and lanes 5–7 are individual biological replicates of total cell lysates of IPF fibroblasts. Loading control depicts Coomassie Blue staining of a representative gel (see Materials and methods). Protein specific lanes from twelve individual immuno-blots show (A) changes seen in protein levels in IPF fibroblasts consistent with genomic alterations identified through the microarray and measured by densitometry (B). ($p<0.05 = ^{*}$, $p<0.01 = ^{**}$, $p<0.001 = ^{***}$).

has focused on cell cycle regulation in these cells. In light of this, we observed that a number of genes associated with the cell cycle and its control were altered in non-cultured IPF fibroblasts. Our findings show altered expression levels in genes promoting the cell cycle progression through the major G1/S check points. For example, the cyclin-dependent kinase inhibitor 2D (*CDKN2D*; p19) is down-regulated, potentially allowing cyclin D1 to promote G1/S progression. In addition we found up-regulation of cell cycle regulators, such as protein regulator of cytokinesis 1 (*PRC1*) and CDC28 protein kinase regulatory subunit 1B (*CKS1B*). Up-regulation of these proteins has been associated with aggressive forms of cancers including multiple myeloma, colorectal, prostate and breast cancer suggesting their potential role in rapid proliferation [37,38]. A number of the disruptions observed in the cell cycle in IPF parallel those observed in various forms of cancer. This correlates histopathologically with the almost "cancer-like" proliferation of fibroblasts and clinically with the progressive course and poor outcomes of IPF. However on the contrary, we also observed down-regulation of members of the cyclin-dependent kinase activating complex (CAK), a powerful pro-cell-cycle regulator, Cyclin H (*CCNH*) and ménage a trois (*MNAT1*). The overall

Table 3
Functional annotation chart: gene ontology term—biological-processes [2].

Gene ontology term	Biological process	Benjamini	Fold enrichment
GO:0016265	Death	3.8E-04	1.6
GO:0040008	Regulation of growth	4.1E-04	2.4
GO:0006950	Response to stress	5.4E-04	1.5
GO:0006928	Cell motility	6.8E-04	1.9
GO:0051674	Localization of cell	6.8E-04	1.9
GO:0007155	Cell adhesion	8.7E-04	1.6
GO:0009719	Response to endogenous stimulus	1.4E-03	1.8
GO:0048468	Cell development	2.0E-03	1.4
GO:0022402	Cell cycle process	2.0E-03	1.6
GO:0016049	Cell growth	3.5E-03	2.1
GO:0008283	Cell proliferation	3.7E-03	1.5
GO:0009605	Response to external stimulus	3.7E-03	1.6
GO:0007049	Cell cycle	3.7E-03	1.5
GO:0065009	Regulation of a molecular function	1.3E-02	1.5
GO:0065008	Regulation of biological quality	3.4E-02	1.4
GO:0009056	Catabolic process	5.8E-02	1.4
GO:0042221	Response to chemical stimulus	6.3E-02	1.4
GO:0051716	Cellular response to stimulus	1.4E-01	3.7
GO:0050817	Coagulation	1.9E-01	2.0
GO:0001775	Cell activation	2.1E-01	1.5
GO:0002520	Immune system development	2.4E-01	1.5

contribution of the CAK complex down-regulation in IPF fibroblasts is currently unclear; however this again underscores the complex nature and potential dysregulation of the cell cycle in IPF.

Cytokine/cytokine receptor signaling

The role of cytokines and cytokine signaling is intuitively central to the pathogenesis of IPF due to their influence on processes such as migration, differentiation and proliferation [23,39]. However, the exact role of many cytokines, specifically in isolated IPF fibroblasts, has yet to be characterized. In this study we observed a complex array of altered cytokine expression in IPF fibroblasts.

C-X-C motif

Within the C-X-C motif cytokine family, we observed up-regulation of the pro-inflammatory pro-platelet basic protein chemokine (C-X-C motif) ligand 7 (*PPBP*). The gene product, PPBP, is known to play a role in the early stages of wound healing through its recruitment of neutrophils to the site of injury, however this cytokine

Table 4
Selected genes from significant biological processes and constituent pathways identified by DAVID analysis of gene ontologies.

Pathway	Genes: increased	Genes: decreased
Protein catabolism (proteasome)	PSMB5, PSMA4, MMP11, PSMA2, USP18, MMP1, PSMA3, PSMD10, MMP2, UBE2T	USP19, USP10
Cytokine/cytokine receptor signaling	BMPR2, ACVR1, TGFB3, INHBA, CD40, KIT, CXCL14, CXCL12, PPBP	IL1R2, RELT TNFRSF14, IFNAR1, IL4R, TNFRSF1A
Cytokine: TGF-beta	RBX1, ID3, ACVR1, INHBA, TGFB3, DCN, COMP, BMPR2	THBS1
Wound healing	BDKRB1, CD40, CXCL12, CXCL14, FN1	STAT3, TNFRSF1A, MMP25, STAT5A
Programmed cell death	FAIM, CD40, DAD1, CCAR1, BAX, CASP6, TNFSF10	DEDD, TNFRSF14, TNFRSF1A, SIPA1, DAPK2, TNFRSF10D
Cell cycle regulation	HDAC2, TGFB3, CDKN3, CKS2	TFDP1, HDAC4, CDKN2D, CCNH, PTEN
ECM/receptor interaction	COL1A1, FN1, SPP1, ITGBL1, THY1, ITGB5	PXN
Vitamin metabolism	NMNAT1, RDH11, RBP1, MDH1	RARA, GLYR1 FOLR3
Wnt pathway	SFRP2, PRICKLE1	DVL1

has also been charged with the ability to recruit mesenchymal stem cells from bone marrow, a role that may contribute directly to increased fibrosis [40]. We also found up-regulation of CXC motif family member, *CXCL12*, which is consistent with this chemokine's potential role in animal models of fibrosis [41–43]. In concert with PPBP, CXCL12 has also the potential to recruit fibrocytes and mesenchymal stem cells (MSC) to the IPF lung, both of which have the capacity to transition to fibroblasts [41,42,44]. Interestingly the theory of recruitment of fibrocytes to the IPF lungs has recently been gaining ground with respect to the pathogenesis of IPF, and circulating levels have been correlated with a poor prognosis [41]. We also identified the up-regulation of the cytokine, *CXCL14,* an orphan chemokine which has not previously been associated with IPF. This cytokine, also known as BRAK (*B*reast *a*nd *K*idney), has been associated with a number of cancers including prostate cancer and pancreatic cancer, where its role varies based on the context of each tissue [45–47]. Pertinent to IPF are recent studies in prostate cancer that explored the role of secreted fibroblast-derived factors in prostate cancer growth [48]. Specifically, it has been demonstrated that tumor associated fibroblasts over-expressing CXCL14 promote the growth of prostate cancer xenografts, increasing tumor angiogenesis and macrophage infiltration. This suggests that CXCL14 is a potential autocrine stimulator of both fibroblast growth and migration, processes central to IPF pathogenesis. CXCL-14 is also believed to prompt enhanced epithelial proliferation, migration and invasion [49,50]. In IPF, these events may enhance the migration of epithelial cells that are undergoing epithelial-to-mesenchymal transition (EMT) and may facilitate the recruitment of cells, such as fibrocytes. These combined multi-modal stimulatory activities make CXCL-14 a potential major player in the cytokine milieu of the IPF lung.

Tumor necrosis factor superfamily

The tumor necrosis factor superfamily (TNFSF), another family of cytokines, was also found to be altered in our IPF fibroblasts. This cytokine family impacts many important regulatory pathways; namely apoptosis, cytoskeletal homeostasis, wound healing, and ECM–receptor interactions (Table 4). In addition to the altered expression of *TNFSF10* and its decoy receptor, *TNFRSF10D,* we also found down-regulation of the pro-inflammatory cytokine, tumor necrosis factor receptor superfamily member 1A (*TNFRSF1A*) (Table 4; Fig. 3C). While the exact contribution of these TNFSF members' alterations in the pathobiology of IPF is unknown, similar transcriptional changes observed in other diseases may shed light on their potential contribution in IPF. For example, while smoking is not considered a cause of IPF, it is a recognized risk factor, and one study has found that *TNFRSF1A* is down-regulated in response to components of cigarette smoke [51] Another change noted was the up-regulation of tumor necrosis factor receptor superfamily, member 5 (*CD40*), which has predominantly been described as a mediator of a broad range of inflammatory responses. However recently, CD40 has been shown to promote fibroblast proliferation in a mouse model of skin fibrosis [52]. Therefore, while CD40 may be pro-inflammatory, it is reasonable to speculate that its action in IPF is more closely akin to its role in the mouse model of skin fibrosis.

TGF-β pathway

The cytokine/cytokine receptor interaction most commonly identified with and critical to the pathogenesis of IPF is that of the TGF-β pathway. This pathway influences many cellular processes, including modulation of apoptosis and cell cycle signaling [23]. Notably, we found that transforming growth factor beta 3 (*TGFB3)* was up-regulated in IPF fibroblasts (Table 3). One potential role for TGFB3 in IPF is its ability to potentiate EMT, a significant process implicated in the pathogenesis of IPF [53–55]. TGFB3 has also been shown to induce an increase in lymphoid enhancer factor 1 (*LEF1*) expression, resulting in the formation of the LEF1/β-catenin complex, which has in turn been shown to initiate EMT [56]. The destruction of the lung epithelium basement membrane, as seen in IPF, enables the direct interaction of epithelial cells with fibroblasts. This disruption of the basement membrane enables factors from the ECM to interface with epithelial cells, thereby promoting their de-differentiation and potential transformation into fibroblasts [54,57,58]. Interestingly, a recent report noted that human lung epithelial cells, in the presence of collagen, release active TGFβ3, which induces EMT via canonical TGFβ signaling [55].

Another TGF-β pathway member we found to be altered was bone morphogenic protein receptor 2, *BMPR2.* Previous studies have associated this receptor with an increased propensity for pulmonary arterial hypertension, and its up-regulation in IPF fibroblasts, might result in the greater predisposition of IPF patients to develop secondary pulmonary hypertension [59]. Clearly, the role of the TGF-β family in IPF is complex and vital, and remains to be fully elucidated.

Defense Response pathway

Our analysis also identified derangements in the pathway of Defense Response processes, which are previously unreported in IPF. Specifically, we found significant up-regulation of Bradykinin Receptor B 1 (*BDKRB1*). The bradykinin ligands, which signal through the two receptors, BDKRB1 and 2, are up-regulated in wounded tissue [60], and may therefore play a role in the limited inflammatory component of IPF. In a recent murine study of kidney fibrosis, a *BDKRB1* knock model showed that the absence of this receptor impeded fibrosis, suggesting that this receptor has pro-fibrotic activity [61]. Therefore, the up-regulation of *BDKRB1* in IPF fibroblasts may similarly play an important fibrogenic role in IPF as suggested in this murine study.

Vitamin metabolism

Novel expression changes in biological processes associated with vitamin metabolism were also noted (Table 3). Among the most prominent were alterations in folate, nicatinamide and retinol metabolism affecting a broad range of biochemical processes, including the citric acid (TCA) cycle. Alterations that influence the TCA cycle can profoundly influence the cellular energetics of a cell and may thereby affect the growth and proliferation of IPF fibroblasts. Specifically, we identified alterations in the expression of a number of members of the retinoic acid pathway. In particular we documented down-regulation of the retinoic acid receptor, alpha (*RARA*) and retinoic acid binding protein (*RBP*) 7 in IPF fibroblasts. RARA is a nuclear receptor mediating the sigõnaling of the powerful morphogen, retinoic acid (RA) and the RBPs all participate in mediating the cellular response to RA. The RA pathway comprises genes shown to be significantly altered in uterine fibroids [62], a common benign neoplasm of smooth muscle cells. The role of altered RA pathway in uterine fibroids may foreshadow the consequences of this pathway's dysregulation in IPF fibroblasts, a cell with similar attributes to smooth muscle cells. In addition, RA has been documented to exacerbate liver fibrosis via plasminogen activator/plasmin levels and induce proteolytic activation of latent transforming growth factor beta (TGF-beta), the purported master cytokine in IPF [63]. Additionally, because of its well described role regulating cellular differentiation during organ development, alterations in the levels of the proteins associated with its pathway, such as those identified herein, may play a fundamental role in the pathobiology of IPF fibroblasts. Intriguingly, the proteasome, whose expression is also altered in these cells, controls the duration of RARA signaling by degradation [64,65].

The up-regulation of nicotinamide nucleotide adenylyltransferase 1 (*NMNAT1*) was also noted in IPF fibroblasts. NMNAT-1 is a central facilitator of redox reactions in the mitochondrial electron transport chain, which influence many cellular processes such as the cell cycle, and catalyzes the formation of the essential cofactor nicotinamide adenine dinucleotide (NAD). Over-expression of NMNAT-1 has been shown to extend the lifespan of cells, an ability which has been attributed to its augmentation of NAD+-dependent histone deacetylation catalyzed by the silent information regulator 2 (Sir2) family of proteins [66]. The Sir2 family, including sirtuin 1 (SIRT1), regulates a variety of cellular processes including differentiation, motility and cell survival [67]. This pro-survival role for NMNAT1, via the Sir2 family in other systems, may have implications for IPF fibroblast longevity. On the contrary, increased NMNAT-1 may play a very different role in IPF fibroblasts. Recent reports have shown that over-expression of NMNAT-1 in HeLa cells modulates the behavior of poly(ADP-ribosyl)ation protein 1 (PARP1) an enzyme essential in processes such as DNA repair and programmed cell death. This association of NMNAT-1 with activated PARP1 can also enhance the relocation of apoptosis inducing factor (AIF) from the mitochondria to the nucleus, thereby triggering apoptosis [68]. This typically occurs in response to oxidant damage mediated through activated PARP1, a pathway which may be an important pro-apoptotic force for IPF fibroblasts [68]. These two contradictory behaviors of NMNAT-1 with respect to cell survival highlight the potential conflicting apoptotic and mitogenic behaviors surrounding IPF fibroblasts [31,32].

In keeping with expression changes that control metabolism, we also demonstrated that malate dehydrogenase I (*MDHI*), which is central to the malate/aspartate shuttle, is also up-regulated [69]. However, it is MDH1 interactions with p53 that may be more pertinent in IPF fibroblast pathobiology. MDH1 has been shown to interact with p53 resulting in regulation of p53 mediated cell cycle arrest and apoptosis [70]. The interactions of MDH1 and p53 are particularly pronounced in environments of low glucose, which may be similar to those of an IPF lung in which aberrant angiogenesis and pathological vascular obliteration might contribute to the decreased availability of glucose to the lung cells [23].

ECM–receptor interactions

The contribution of the ECM produced by the fibroblast is central to the phenotype of the IPF lung and its clinical, radiographic and histopathologic manifestations. As expected, our analysis identified the up-regulation of *COL1A1*, the ECM component whose deposition is the hallmark of pulmonary fibrosis. This up-regulation occurred in concert with the up-regulation of *COL16A1,* a member of the fibril-associated collagens with interrupted helices (FACIT) family. This co-expression increase may serve to strengthen the integrity of the evolving fibroblasts' ECM, promoting the adhesion and fibrogenic nature of the IPF fibroblast. This is similar to the situation in glioblastomas where increased *COL16A1* expression has been shown to contribute to the increased adhesion of these cells [71]. It is also possible that the up-regulation of *COL6A2* observed in our IPF fibroblasts may facilitate increased interactions between fibronectin (FN) and its integrin receptors thereby increasing its fibrogenic effect [72]. FN1 is known for its role in cell adhesion and migration processes, particularly in wound healing (Table 3). In keeping with these hypothesis is the finding that fibronectin 1 (*FN1*) was also up-regulated in IPF fibroblasts. In addition, our study identified a multitude of other up-regulated collagen subtypes, including *COL5A2* and *COL3A1,* which are known to interact with Col1A1 contributing to the classic IPF ECM [72].

We also noted the up-regulation of non-collagenous constituents of the ECM. The most prominent of which are the laminin family of glycoproteins, including laminin β 2 (*LAMB2*) and laminin α 4 (*LAMA4*), both of which were up-regulated. Laminins are of particular importance as they are integral to the basement membrane, and modulate intercellular adhesion and cellular motility [73]. While it is unknown how the up-regulation of *LAMB2* contributes to IPF pathobiology, this ECM component has previously been associated with cell adhesion, differentiation, migration, signaling of neurite outgrowth and prostate cancer metastasis [74]. Of these processes, cell adhesion, differentiation and migration have all been identified as important factors in fibrogenesis, and therefore by analogy suggest a potential contribution of LAMB2 up-regulation to the fibrotic phenotype of IPF [75].

The matricellular family of proteins is a class of ECM molecules whose properties are distinct from both the structural macromolecules and the more bioactive proteins such as growth factors, cytokines, and proteases that also comprise the ECM. They are defined by their ability to modulate cell–matrix interactions and are actively expressed during wound repair and disease [76]. This family, highly represented in our gene list, includes, tenascin-C (TNC), osteopontin (SPP1), secreted protein acidic rich in cysteine (SPARC), bone sialoprotein, thrombospondins and members of the CCN family such as cysteine-rich, angiogenic inducer, 61 (CYR61; CCN1). While the roles of tenascin-C, SPARC, SPP1,thrombospondins and CYR61 have previously been explored in pulmonary fibrosis, the role of altered *POSTN* (periostin) expression has yet to be clarified.

Periostin affects structural and functional properties of connective tissues by influencing collagen fibrillogenesis [76]. However, its reported function as a novel component of subepithelial fibrosis in bronchial asthma [77] may allude to a similar role in IPF. *POSTN* is also up-regulated in the stromal cells of bone marrow fibrosis, and this up-regulation is enhanced by the presence of TGF-β, making periostin a particularly interesting component of IPF [78]. Increased expression of *POSTN* has also been noted in cancer studies where certain of its actions might be consistent with IPF pathogenic mechanisms, such as the stimulation of angiogenesis [79]. It achieves this via increased expression of the VEGF receptor Flk-1/KDR by endothelial cells [80]. Periostin has also demonstrated a role in EMT, a process of great importance in IPF [4]. The role of the ECM and the components thereof are clearly crucial to IPF disease progression as evidenced by the aforementioned individual components and their documented interplay and behaviors in other fibrotic diseases.

Wnt pathway

A pathway with rapidly emerging implications in IPF is the Wnt pathway [24–26]. The Wnt pathway coordinates with many cellular regulatory processes including cell cycle regulation, TGF-β signaling, and proteasomal regulation of protein degradation. Wnt signaling has also been shown to be increased in IPF epithelial cells, IPF whole lung tissue samples and primary fibroblasts cultured from lung tissue [24–26]. While the exact role of Wnt signaling in IPF requires greater clarification, it is clear that downstream target genes of the Wnt pathway might play a significant role in IPF. Specifically in this study we demonstrate alteration of 11 genes within the Wnt pathway including the down-regulation of dishevelled (*DVL1)* and the up-regulation of *SFRP2*, indicating aberrant Wnt signaling in IPF fibroblasts. SFRP2 is of particular interest as it is not only an antagonist of the Wnt signaling pathway but it has also recently been identified as contributing to fibrosis in a mouse model of myocardial infarction. This fibrotic behavior is associated with SFRP2's ability to act as a procollagen C proteinase enhancer, which enhances the conversion of procollagen (I–III) precursors into major fibrillar components of the ECM through the activity of the mammalian tolloid-like proteinases [81]. Two additional procollagen remodeling genes were also found to be up-regulated in our IPF fibroblasts: procollagen C-endopeptidase enhancer (*PCOLCE*) and

prolyl 4-hydroxylase, alpha polypeptide II (*P4HA2*). Both contribute to and enhance the processing and correct folding of collagen in the ECM. With their inherent role in ECM integrity, these proteinases and enhancers of proteinases may potentially prove to be valuable targets for future therapies in IPF.

Cytoskeletal organization and biogenesis

Changes in biological process associated with cytoskeletal organization and biogenesis are also central to IPF fibroblast pathobiology. While increased α-SMA in IPF fibroblasts is expected (Fig. 4), our study also demonstrates previously unidentified expression changes in genes associated with cytoskeletal organization and biogenesis. Specifically, we found basic calponin (*CNN1*), a modulator of the cytoskeleton, to be highly up-regulated. CNN1 is involved in host–tumor interactions where it has been shown to facilitate smooth muscle migration [82], a role that may also be important in IPF fibroblasts. A second calponin family member, neutral calponin (*CNN2*), was found to be down-regulated in the IPF fibroblast. Unlike CNN1, CNN2 has been shown to inhibit the activity of the actin cytoskeleton *in vitro* by inhibiting cellular contractile capabilities [83] and by modulating cell proliferation through the inhibition of cytokinesis [84]. Its down-regulation, as seen in IPF fibroblasts, could result in a decrease of its inhibition of cell proliferation, and thereby contribute to the abundance of fibroblasts.

Conclusions

Our technique in providing a genomic analysis of rapidly isolated non-cultured fibroblasts from IPF lungs limits the opportunity for *ex vivo* phenotypic transformation and thereby provides a unique insight into this central IPF effector cell [15–17]. Previous studies utilizing whole lung tissue have provided a global spectrum of gene signaling. However, important expression changed specific to particular cells and critical to disease pathogenesis may be lost in the genomic milieu of total lung tissue as a result of signal-dilution. Our methodology has provided a conduit to uncover previously unidentified pathways and components that may be critical to our understanding of the uninhibited proliferation, excessive ECM deposition and aberrant apoptosis that characterize the IPF fibroblast.

A potential limitation of our study is the choice of patients enrolled which included only those with end-stage disease. It is therefore possible that our analysis of the pathways and mechanisms may not be representative of the fibroblasts in patients with earlier stages of the disease. Additionally, for a number of reasons we chose not to use laser capture microdissection (LCM) to isolate the fibroblast population. First, the multiple sources of the fibroblast population in IPF make identifying fibroblasts for LCM problematic. In addition, there is a lack of a truly specific cell marker for fibroblasts. The specific make-up of the fibroblast population in the IPF lung remains unclear with four possible reservoirs contributing to the overall fibroblast population including circulating fibrocytes, de-differentiated epithelial cells, pleural mesothelial cells and resident activated fibroblasts [41,54,85,86]. Therefore use of LCM to selectively remove fibroblastic foci may be too restrictive in its selection of fibroblasts for this type of study. For example, it may exclude contributing fibroblasts outside of the developed foci, such as those residing at the edges of normal appearing tissue or adjacent to vasculature or airways. Lastly, LCM cannot capture live cells from tissue, thereby restricting further experimentation.

By exploiting the differential binding capacity of fibroblasts, we were able to isolate our IPF fibroblasts and identify global genomic differences in comparison to identically processed normal controls. These differences included expression changes highly enriched in biological processes previously unreported in IPF. In particular, the alterations in vitamin metabolic processes deserve further scrutiny as 12these processes impact fundamental homeostatic processes including cellular energetics and the TCA cycle, cellular differentiation, apoptosis and the cell cycle. In addition, our observations of expression changes within numerous constituents of the ubiquitin/proteasomal degradation pathway suggest that further characterization of this regulatory process is warranted.

In conclusion, our data help to shed light on potential biological processes and pathways that might be important in explaining the unchecked abundance of fibroblasts that characterizes IPF. Whatever the trigger or predisposing factor(s) might be, it appears that "switching off" this cell could be integral to halting the course of the disease and improving patient outcomes. Our study provides a genomic foundation for in-depth functional studies that will hopefully enable the development of future, therapeutic trials targeting this central effector cell.

Appendix A. Supplementary data

Supplementary data associated with this article can be found, in the online version, at doi:10.1016/j.ygeno.2010.04.005.

References

[1] O.J. Dempsey, Clinical review: idiopathic pulmonary fibrosis—past, present and future, Respir. Med. 100 (2006) 1871–1885.
[2] C.J. Scotton, R.C. Chambers, Molecular targets in pulmonary fibrosis: the myofibroblast in focus, Chest 132 (2007) 1311–1321.
[3] M. Selman, A. Pardo, L. Barrera, A. Estrada, S.R. Watson, K. Wilson, N. Aziz, N. Kaminski, A. Zlotnik, Gene expression profiles distinguish idiopathic pulmonary fibrosis from hypersensitivity pneumonitis, Am. J. Respir. Crit. Care Med. 173 (2006) 188–198.
[4] I.V. Yang, L.H. Burch, M.P. Steele, J.D. Savov, J.W. Hollingsworth, E. McElvania-Tekippe, K.G. Berman, M.C. Speer, T.A. Sporn, K.K. Brown, M.I. Schwarz, D.A. Schwartz, Gene expression profiling of familial and sporadic interstitial pneumonia, Am. J. Respir. Crit. Care Med. 175 (2007) 45–54.
[5] J. Wang, H. Chen, A. Seth, C.A. McCulloch, Mechanical force regulation of myofibroblast differentiation in cardiac fibroblasts, Am. J. Physiol. Heart Circ. Physiol. 285 (2003) H1871–H1881.
[6] A.I. Saeed, V. Sharov, J. White, J. Li, W. Liang, N. Bhagabati, J. Braisted, M. Klapa, T. Currier, M. Thiagarajan, A. Sturn, M. Snuffin, A. Rezantsev, D. Popov, A. Ryltsov, E. Kostukovich, I. Borisovsky, Z. Liu, A. Vinsavich, V. Trush, J. Quackenbush, TM4: a free, open-source system for microarray data management and analysis, Biotechniques 34 (2003) 374–378.
[7] W.S. Cleveland, S.J. Devlin, Locally weighted regression: an approach to regression analysis by local fitting, American Statistical Association, 1988, pp. 596–610.
[8] V.G. Tusher, R. Tibshirani, G. Chu, Significance analysis of microarrays applied to the ionizing radiation response, Proc. Natl Acad. Sci. USA 98 (2001) 5116–5121.
[9] M.W. Pfaffl, A new mathematical model for relative quantification in real-time RT-PCR, Nucleic Acids Res. 29 (2001) e45.
[10] W. Huang da, B.T. Sherman, R.A. Lempicki, Systematic and integrative analysis of large gene lists using DAVID bioinformatics resources, Nat. Protoc. 4 (2009) 44–57.
[11] G. Dennis Jr., B.T. Sherman, D.A. Hosack, J. Yang, W. Gao, H.C. Lane, R.A. Lempicki, DAVID: Database for Annotation, Visualization, and Integrated Discovery, Genome Biol. 4 (2003) P3.
[12] M. Kanehisa, S. Goto, M. Hattori, K.F. Aoki-Kinoshita, M. Itoh, S. Kawashima, T. Katayama, M. Araki, M. Hirakawa, From genomics to chemical genomics: new developments in KEGG, Nucleic Acids Res. 34 (2006) D354–D357.
[13] M. Kanehisa, S. Goto, KEGG: Kyoto Encyclopedia of Genes and Genomes, Nucleic Acids Res. 28 (2000) 27–30.
[14] M. Kanehisa, S. Goto, M. Furumichi, M. Tanabe, M. Hirakawa, KEGG for representation and analysis of molecular networks involving diseases and drugs, Nucleic Acids Res. 38 (2010) D355–D360.
[15] G. Elaut, T. Henkens, P. Papeleu, S. Snykers, M. Vinken, T. Vanhaecke, V. Rogiers, Molecular mechanisms underlying the dedifferentiation process of isolated hepatocytes and their cultures, Curr. Drug Metab. 7 (2006) 629–660.
[16] F. Pampaloni, E.G. Reynaud, E.H. Stelzer, The third dimension bridges the gap between cell culture and live tissue, Nat. Rev. Mol. Cell Biol. 8 (2007) 839–845.
[17] C. Guidry, Isolation and characterization of porcine Muller cells. Myofibroblastic dedifferentiation in culture, Invest. Ophthalmol. Vis. Sci. 37 (1996) 740–752.
[18] T.D. Starner, N. Zhang, G. Kim, M.A. Apicella, P.B. McCray Jr., Haemophilus influenzae forms biofilms on airway epithelia: implications in cystic fibrosis, Am. J. Respir. Crit. Care Med. 174 (2006) 213–220.
[19] P.H. Karp, T.O. Moninger, S.P. Weber, T.S. Nesselhauf, J.L. Launspach, J. Zabner, M.J. Welsh, An in vitro model of differentiated human airway epithelia. Methods for establishing primary cultures, Meth. Mol. Biol. 188 (2002) 115–137.

[20] M. Korfei, C. Ruppert, P. Mahavadi, I. Henneke, P. Markart, M. Koch, G. Lang, L. Fink, R.M. Bohle, W. Seeger, T.E. Weaver, A. Guenther, Epithelial endoplasmic reticulum stress and apoptosis in sporadic idiopathic pulmonary fibrosis, Am. J. Respir. Crit. Care Med. 178 (2008) 838–846.
[21] J.M. Purkerson, R.S. Smith, S.J. Pollock, R.P. Phipps, The TRAF6, but not the TRAF2/3, binding domain of CD40 is required for cytokine production in human lung fibroblasts, Eur. J. Immunol. 35 (2005) 2920–2928.
[22] G.D. Sempowski, P.R. Chess, R.P. Phipps, CD40 is a functional activation antigen and B7-independent T cell costimulatory molecule on normal human lung fibroblasts, J. Immunol. 158 (1997) 4670–4677.
[23] T.A. Wynn, Cellular and molecular mechanisms of fibrosis, J. Pathol. 214 (2008) 199–210.
[24] M. Konigshoff, N. Balsara, E.M. Pfaff, M. Kramer, I. Chrobak, W. Seeger, O. Eickelberg, Functional Wnt signaling is increased in idiopathic pulmonary fibrosis, PLoS ONE 3 (2008) e2142.
[25] L.J. Vuga, A. Ben-Yehudah, E. Kovkarova-Naumovski, T. Oriss, K.F. Gibson, C. Feghali-Bostwick, N. Kaminski, WNT5A is a regulator of fibroblast proliferation and resistance to apoptosis, Am. J. Respir. Cell Mol. Biol. 41 (2009) 583–589.
[26] M. Chilosi, V. Poletti, A. Zamo, M. Lestani, L. Montagna, P. Piccoli, S. Pedron, M. Bertaso, A. Scarpa, B. Murer, A. Cancellieri, R. Maestro, G. Semenzato, C. Doglioni, Aberrant Wnt/beta-catenin pathway activation in idiopathic pulmonary fibrosis, Am. J. Pathol. 162 (2003) 1495–1502.
[27] A. Pardo, K. Gibson, J. Cisneros, T.J. Richards, Y. Yang, C. Becerril, S. Yousem, I. Herrera, V. Ruiz, M. Selman, N. Kaminski, Up-regulation and profibrotic role of osteopontin in human idiopathic pulmonary fibrosis, PLoS Med. 2 (2005) e251.
[28] A.M. Sousa, T. Liu, O. Guevara, J. Stevens, B.L. Fanburg, M. Gaestel, D. Toksoz, U.S. Kayyali, Smooth muscle alpha-actin expression and myofibroblast differentiation by TGFbeta are dependent upon MK2, J. Cell. Biochem. 100 (2007) 1581–1592.
[29] P.D. Arora, K.J. Bibby, C.A. McCulloch, Slow oscillations of free intracellular calcium ion concentration in human fibroblasts responding to mechanical stretch, J. Cell. Physiol. 161 (1994) 187–200.
[30] S.L. Vyalov, G. Gabbiani, Y. Kapanci, Rat alveolar myofibroblasts acquire alpha-smooth muscle actin expression during bleomycin-induced pulmonary fibrosis, Am. J. Pathol. 143 (1993) 1754–1765.
[31] V.J. Thannickal, J.C. Horowitz, Evolving concepts of apoptosis in idiopathic pulmonary fibrosis, Proc. Am. Thorac. Soc. 3 (2006) 350–356.
[32] C. Ramos, M. Montano, J. Garcia-Alvarez, V. Ruiz, B.D. Uhal, M. Selman, A. Pardo, Fibroblasts from idiopathic pulmonary fibrosis and normal lungs differ in growth rate, apoptosis, and tissue inhibitor of metalloproteinases expression, Am. J. Respir. Cell Mol. Biol. 24 (2001) 591–598.
[33] C.L. Fattman, Apoptosis in pulmonary fibrosis: too much or not enough? Antioxid. Redox Signal. 10 (2008) 379–385.
[34] A. Pardo, M. Selman, N. Kaminski, Approaching the degradome in idiopathic pulmonary fibrosis, Int. J. Biochem. Cell Biol. 40 (2008) 1141–1155.
[35] M.H. Glickman, A. Ciechanover, The ubiquitin–proteasome proteolytic pathway: destruction for the sake of construction, Physiol. Rev. 82 (2002) 373–428.
[36] S.I. Reed, The ubiquitin–proteasome pathway in cell cycle control, Results Probl. Cell Differ. 42 (2006) 147–181.
[37] T. Hattori, K. Kitagawa, C. Uchida, T. Oda, M. Kitagawa, Cks1 is degraded via the ubiquitin–proteasome pathway in a cell cycle-dependent manner, Genes Cells 8 (2003) 889–896.
[38] A. Shimo, T. Nishidate, T. Ohta, M. Fukuda, Y. Nakamura, T. Katagiri, Elevated expression of protein regulator of cytokinesis 1, involved in the growth of breast cancer cells, Cancer Sci. 98 (2007) 174–181.
[39] B.D. Bringardner, C.P. Baran, T.D. Eubank, C.B. Marsh, The role of inflammation in the pathogenesis of idiopathic pulmonary fibrosis, Antioxid. Redox Signal. 10 (2008) 287–301.
[40] G. Kalwitz, M. Endres, K. Neumann, K. Skriner, J. Ringe, O. Sezer, M. Sittinger, T. Haupl, C. Kaps, Gene expression profile of adult human bone marrow-derived mesenchymal stem cells stimulated by the chemokine CXCL7, Int. J. Biochem. Cell Biol. 41 (2009) 649–658.
[41] A. Andersson-Sjoland, C.G. de Alba, K. Nihlberg, C. Becerril, R. Ramirez, A. Pardo, G. Westergren-Thorsson, M. Selman, Fibrocytes are a potential source of lung fibroblasts in idiopathic pulmonary fibrosis, Int. J. Biochem. Cell Biol. 40 (2008) 2129–2140.
[42] J. Xu, A. Mora, H. Shim, A. Stecenko, K.L. Brigham, M. Rojas, Role of the SDF-1/CXCR4 axis in the pathogenesis of lung injury and fibrosis, Am. J. Respir. Cell Mol. Biol. 37 (2007) 291–299.
[43] Y. Yang, L. Zou, M. Li, Y. Zhao, CXCL12/CXCR4 expression in trophoblasts takes part in materno-fetal immune tolerance and vascular remodeling, J. Huazhong Univ. Sci. Technol. Med. Sci. 26 (2006) 466–468.
[44] R.J. Phillips, M.D. Burdick, K. Hong, M.A. Lutz, L.A. Murray, Y.Y. Xue, J.A. Belperio, M.P. Keane, R.M. Strieter, Circulating fibrocytes traffic to the lungs in response to CXCL12 and mediate fibrosis, J. Clin. Invest. 114 (2004) 438–446.
[45] S.R. Schwarze, J. Luo, W.B. Isaacs, D.F. Jarrard, Modulation of CXCL14 (BRAK) expression in prostate cancer, Prostate 64 (2005) 67–74.
[46] G.V. Shurin, R.L. Ferris, I.L. Tourkova, L. Perez, A. Lokshin, L. Balkir, B. Collins, G.S. Chatta, M.R. Shurin, Loss of new chemokine CXCL14 in tumor tissue is associated with low infiltration by dendritic cells (DC), while restoration of human CXCL14 expression in tumor cells causes attraction of DC both in vitro and in vivo, J. Immunol. 174 (2005) 5490–5498.
[47] M.N. Wente, C. Mayer, M.M. Gaida, C.W. Michalski, T. Giese, F. Bergmann, N.A. Giese, M.W. Buchler, H. Friess, CXCL14 expression and potential function in pancreatic cancer, Cancer Lett. 259 (2008) 209–217.
[48] M. Augsten, C. Hagglof, E. Olsson, C. Stolz, P. Tsagozis, T. Levchenko, M.J. Frederick, A. Borg, P. Micke, L. Egevad, A. Ostman, CXCL14 is an autocrine growth factor for fibroblasts and acts as a multi-modal stimulator of prostate tumor growth, Proc. Natl Acad. Sci. USA 106 (2009) 3414–3419.
[49] M.J. Frederick, Y. Henderson, X. Xu, M.T. Deavers, A.A. Sahin, H. Wu, D.E. Lewis, A. K. El-Naggar, G.L. Clayman, In vivo expression of the novel CXC chemokine BRAK in normal and cancerous human tissue, Am. J. Pathol. 156 (2000) 1937–1950.
[50] M. Allinen, R. Beroukhim, L. Cai, C. Brennan, J. Lahti-Domenici, H. Huang, D. Porter, M. Hu, L. Chin, A. Richardson, S. Schnitt, W.R. Sellers, K. Polyak, Molecular characterization of the tumor microenvironment in breast cancer, Cancer Cell 6 (2004) 17–32.
[51] S.H. Sohn, K.N. Kim, I.K. Kim, E.I. Lee, J.J. Ryu, M.K. Kim, Effects of tobacco compounds on gene expression in fetal lung fibroblasts, Environ. Toxicol. 23 (2008) 423–434.
[52] K. Komura, M. Fujimoto, K. Yanaba, T. Matsushita, Y. Matsushita, M. Horikawa, F. Ogawa, K. Shimizu, M. Hasegawa, K. Takehara, S. Sato, Blockade of CD40/CD40 ligand interactions attenuates skin fibrosis and autoimmunity in the tight-skin mouse, Ann. Rheum. Dis. 67 (2008) 867–872.
[53] B.D. Uhal, J.K. Kim, X. Li, M. Molina-Molina, Angiotensin-TGF-beta 1 crosstalk in human idiopathic pulmonary fibrosis: autocrine mechanisms in myofibroblasts and macrophages, Curr. Pharm. Des. 13 (2007) 1247–1256.
[54] B.C. Willis, Z. Borok, TGF-beta-induced EMT: mechanisms and implications for fibrotic lung disease, Am. J. Physiol. Lung Cell. Mol. Physiol. 293 (2007) L525–L534.
[55] Y. Shintani, Y. Fukumoto, N. Chaika, R. Svoboda, M.J. Wheelock, K.R. Johnson, Collagen I-mediated up-regulation of N-cadherin requires cooperative signals from integrins and discoidin domain receptor 1, J. Cell Biol. 180 (2008) 1277–1289.
[56] D. Medici, E.D. Hay, B.R. Olsen, Snail and Slug promote epithelial–mesenchymal transition through beta-catenin-T-cell factor-4-dependent expression of transforming growth factor-beta3, Mol. Biol. Cell 19 (2008) 4875–4887.
[57] M. Selman, A. Pardo, Idiopathic pulmonary fibrosis: an epithelial/fibroblastic cross-talk disorder, Respir. Res. 3 (2002) 3.
[58] M. Selman, T.E. King, A. Pardo, Idiopathic pulmonary fibrosis: prevailing and evolving hypotheses about its pathogenesis and implications for therapy, Ann. Intern. Med. 134 (2001) 136–151.
[59] J. West, K. Fagan, W. Steudel, B. Fouty, K. Lane, J. Harral, M. Hoedt-Miller, Y. Tada, J. Ozimek, R. Tuder, D.M. Rodman, Pulmonary hypertension in transgenic mice expressing a dominant-negative BMPRII gene in smooth muscle, Circ. Res. 94 (2004) 1109–1114.
[60] Y.M. Kim, E.S. Jeon, M.R. Kim, J.S. Lee, J.H. Kim, Bradykinin-induced expression of alpha-smooth muscle actin in human mesenchymal stem cells, Cell. Signal. 20 (2008) 1882–1889.
[61] P.H. Wang, M.A. Cenedeze, G. Campanholle, D.M. Malheiros, H.A. Torres, J.B. Pesquero, A. Pacheco-Silva, N.O. Camara, Deletion of bradykinin B1 receptor reduces renal fibrosis, Int. Immunopharmacol. 9 (2009) 653–657.
[62] M. Zaitseva, B.J. Vollenhoven, P.A. Rogers, Retinoic acid pathway genes show significantly altered expression in uterine fibroids when compared with normal myometrium, Mol. Hum. Reprod. 13 (2007) 577–585.
[63] M. Okuno, S. Kojima, K. Akita, R. Matsushima-Nishiwaki, S. Adachi, T. Sano, Y. Takano, K. Takai, A. Obora, I. Yasuda, Y. Shiratori, Y. Okano, J. Shimada, Y. Suzuki, Y. Muto, Y. Moriwaki, Retinoids in liver fibrosis and cancer, Front. Biosci. 7 (2002) d204–d218.
[64] G. Bour, S. Lalevee, C. Rochette-Egly, Protein kinases and the proteasome join in the combinatorial control of transcription by nuclear retinoic acid receptors, Trends Cell Biol. 17 (2007) 302–309.
[65] J. Bastien, C. Rochette-Egly, Nuclear retinoid receptors and the transcription of retinoid-target genes, Gene 328 (2004) 1–16.
[66] T. Zhang, W.L. Kraus, SIRT1-dependent regulation of chromatin and transcription: Linking NAD(+) metabolism and signaling to the control of cellular functions, Biochim. Biophys. Acta 1804 (2009) 1666–1675.
[67] S. Michan, D. Sinclair, Sirtuins in mammals: insights into their biological function, Biochem. J. 404 (2007) 1–13.
[68] F. Berger, C. Lau, M. Ziegler, Regulation of poly(ADP-ribose) polymerase 1 activity by the phosphorylation state of the nuclear NAD biosynthetic enzyme NMN adenylyl transferase 1, Proc. Natl Acad. Sci. USA 104 (2007) 3765–3770.
[69] A.S. Lo, C.T. Liew, S.M. Ngai, S.K. Tsui, K.P. Fung, C.Y. Lee, M.M. Waye, Developmental regulation and cellular distribution of human cytosolic malate dehydrogenase (MDH1), J. Cell. Biochem. 94 (2005) 763–773.
[70] S.M. Lee, J.H. Kim, E.J. Cho, H.D. Youn, A nucleocytoplasmic malate dehydrogenase regulates p53 transcriptional activity in response to metabolic stress, Cell Death Differ. 16 (2009) 738–748.
[71] V. Senner, S. Ratzinger, S. Mertsch, S. Grassel, W. Paulus, Collagen XVI expression is upregulated in glioblastomas and promotes tumor cell adhesion, FEBS Lett. 582 (2008) 3293–3300.
[72] A. Kassner, K. Tiedemann, H. Notbohm, T. Ludwig, M. Morgelin, D.P. Reinhardt, M.L. Chu, P. Bruckner, S. Grassel, Molecular structure and interaction of recombinant human type XVI collagen, J. Mol. Biol. 339 (2004) 835–853.
[73] S. Scheele, A. Nystrom, M. Durbeej, J.F. Talts, M. Ekblom, P. Ekblom, Laminin isoforms in development and disease, J. Mol. Med. 85 (2007) 825–836.
[74] S. Ashida, H. Nakagawa, T. Katagiri, M. Furihata, M. Iizumi, Y. Anazawa, T. Tsunoda, R. Takata, K. Kasahara, T. Miki, T. Fujioka, T. Shuin, Y. Nakamura, Molecular features of the transition from prostatic intraepithelial neoplasia (PIN) to prostate cancer: genome-wide gene-expression profiles of prostate cancers and PINs, Cancer Res. 64 (2004) 5963–5972.
[75] X. Huang, G. Ji, Y. Wu, B. Wan, L. Yu, LAMA4, highly expressed in human hepatocellular carcinoma from Chinese patients, is a novel marker of tumor invasion and metastasis, J. Cancer Res. Clin. Oncol. 134 (2008) 705–714.

[76] D.W. Hamilton, Functional role of periostin in development and wound repair: implications for connective tissue disease, J. Cell Commun. Signal 2 (2008) 9–17.
[77] G. Takayama, K. Arima, T. Kanaji, S. Toda, H. Tanaka, S. Shoji, A.N. McKenzie, H. Nagai, T. Hotokebuchi, K. Izuhara, Periostin: a novel component of subepithelial fibrosis of bronchial asthma downstream of IL-4 and IL-13 signals, J. Allergy Clin. Immunol. 118 (2006) 98–104.
[78] E. Oku, T. Kanaji, Y. Takata, K. Oshima, R. Seki, S. Morishige, R. Imamura, K. Ohtsubo, M. Hashiguchi, K. Osaki, K. Yakushiji, K. Yoshimoto, H. Ogata, H. Hamada, K. Izuhara, M. Sata, T. Okamura, Periostin and bone marrow fibrosis, Int. J. Hematol. 88 (2008) 57–63.
[79] I. Takanami, T. Abiko, S. Koizumi, Expression of periostin in patients with non-small cell lung cancer: correlation with angiogenesis and lymphangiogenesis, Int. J. Biol. Markers 23 (2008) 182–186.
[80] R. Shao, S. Bao, X. Bai, C. Blanchette, R.M. Anderson, T. Dang, M.L. Gishizky, J.R. Marks, X.F. Wang, Acquired expression of periostin by human breast cancers promotes tumor angiogenesis through up-regulation of vascular endothelial growth factor receptor 2 expression, Mol. Cell. Biol. 24 (2004) 3992–4003.
[81] K. Kobayashi, M. Luo, Y. Zhang, D.C. Wilkes, G. Ge, T. Grieskamp, C. Yamada, T.C. Liu, G. Huang, C.T. Basson, A. Kispert, D.S. Greenspan, T.N. Sato, Secreted Frizzled-related protein 2 is a procollagen C proteinase enhancer with a role in fibrosis associated with myocardial infarction, Nat. Cell Biol. 11 (2009) 46–55.
[82] H. Yamamura, N. Hirano, H. Koyama, Y. Nishizawa, K. Takahashi, Loss of smooth muscle calponin results in impaired blood vessel maturation in the tumor–host microenvironment, Cancer Sci. 98 (2007) 757–763.
[83] Y. Fukui, H. Masuda, M. Takagi, K. Takahashi, K. Kiyokane, The presence of h2-calponin in human keratinocyte, J. Dermatol. Sci. 14 (1997) 29–36.
[84] M.M. Hossain, D.Y. Hwang, Q.Q. Huang, Y. Sasaki, J.P. Jin, Developmentally regulated expression of calponin isoforms and the effect of h2-calponin on cell proliferation, Am. J. Physiol. Cell Physiol. 284 (2003) C156–C167.
[85] O. Larsson, D. Diebold, D. Fan, M. Peterson, R.S. Nho, P.B. Bitterman, C.A. Henke, Fibrotic myofibroblasts manifest genome-wide derangements of translational control, PLoS ONE 3 (2008) e3220.
[86] F. Nasreen, N. Altaf Malik, M. Naeem Riaz, J. Anver Qureshi, Detection and screening of bovine leukocyte adhesion deficiency in Pakistan using molecular methods, Hereditas 146 (2009) 74–78.